ELSEVIER

Biochimica et Biophysica Acta 1252 (1995) 95–102

BBA Biochimica et Biophysica Acta

The thermodynamics of association and unfolding of the 205–316 C-terminal fragment of thermolysin

Ana I. Azuaga [a], Francisco Conejero-Lara [a], Germán Rivas [b], Vincenzo De Filippis [c], Angelo Fontana [c], Pedro L. Mateo [a,*]

[a] *Departamento de Química Física, Facultad de Ciencias, e Instituto de Biotecnología, Universidad de Granada, 18071 Granada, Spain*
[b] *Centro de Investigaciones Biológicas, CSIC, Velazquez 144, 28006 Madrid, Spain*
[c] *CRIBI Biotechnology Center, University of Padua, 35121 Padua, Italy*

Received 20 February 1995; accepted 23 May 1995

Abstract

The 205–316 C-terminal fragment of thermolysin has been studied by differential scanning calorimetry at pH values 2.5, 3.0, 3.5, 4.0 and 5.0 and at a constant ionic strength of 130 mM. The thermal unfolding of the fragment occurs at thermodynamic equilibrium under our experimental conditions. The effect of sample concentration at the different pH values on the calorimetric traces is consistent with a monomer-dimer equilibrium of the folded fragment, which undergoes thermal unfolding into individual fragments. Equilibrium sedimentation experiments at 10°C and different pH values confirm the presence of the association equilibrium and provide the value of the dimerization constants. The global analysis of the calorimetric, heat capacity curves has been carried out by a multidimensional fitting to the model $N_2 \rightleftharpoons 2N \rightleftharpoons 2U$. The analysis leads to a complete thermodynamic characterization of both the association and unfolding processes of the fragment. The resulting thermodynamic functions suggest a partially unfolded structure for both the monomeric and dimeric fragment, as well as a conformational change linked to the association process. Our results are discussed in terms of the structural information currently available and compared with the energetics of unfolding of the shorter 255–316 dimeric C-terminal fragment of thermolysin (Conejero-Lara, F., De Filippis, V., Fontana, A. and Mateo, P.L. (1994) FEBS Lett. 344, 154–156). The presence of the additional 50 residues increases the relative population of the 205–316 monomeric fragment versus that of the 255–316 fragment.

Keywords: Protein domain; Domain folding; Domain stability; DSC; Analytical ultracentrifuge

1. Introduction

Co-operative non-covalent interactions play the crucial role in both protein folding and protein-protein recognition. The stability of the folded protein or the protein complex thus comes from the interplay of this interaction network, including the changes in the exposure of polar and non-polar protein surfaces to the solvent. In fact, protein associations are quite often coupled to modifications in the folding content of the interacting monomeric subunits [1].

Protein folding, stability and assembly is a central problem in present-day molecular biology, where the study of peptide model compounds is a logical approach to rationalize some of its structural and energetic aspects. Peptide models are of particular interest when they correspond to isolated protein regions capable of folding in solution, i.e., submolecular co-operative domains. Thus, it is known that proteins above a certain size (around 100 amino-acid residues) are frequently composed of folding domains [2]. The thermodynamic study of these cooperative units can be of valuable interest to characterize the energetics of both the early stages in protein folding and the possible association of these units in solution when isolated from the rest of the protein.

Thermolysin is a well-characterized metalloproteinase of 316 amino-acid residues from *Bacillus thermoproteolyticus rokko*, which consist of two similar structural domains, 1–157 and 158–316 [3,4]. Considerable work has been done on the isolation and definition of different submolecular domains of the enzyme, which are able to adopt a globular conformation in solution as well as to undergo cooperative unfolding transitions under the appro-

* Corresponding author. E-mail: pmateo@ugr.es. Fax: +34 58 274258.

SSDI 0167-4838(95)00129-8

priate conditions [5–9]. We have recently reported a calorimetric study of the unfolding of the 255–316 C-terminal fragment of thermolysin [10]. This shorter fragment, which is a dimer at above 0.4 mg/ml [11] with three native-like α-helices per monomer, as shown by NMR studies [12], follows an $N_2 \rightleftharpoons 2U$ two-state unfolding process.

We have studied here the thermodynamics of the folded 205–316 C-terminal fragment of thermolysin by differential scanning calorimetry (DSC) at five pH values within the range 2.5–5.0. The thermal unfolding of this fragment, which contains a four α-helix bundle in native thermolysin, has proved to occur under equilibrium conditions. The effect of concentration on the DSC endotherms is consistent with a folded monomer-dimer equilibrium, which unfolds into individual monomers on increasing temperature. Equilibrium sedimentation experiments at 10°C and different pH values have confirmed the dimerization equilibrium of the fragment and allowed us to obtain the association constants. We have made a global analysis of the experimental heat capacity curves, leading to a complete energetic characterization of the dissociation and unfolding processes. The thermodynamic parameters obtained are discussed in the light of the structural information available and compared with those previously obtained for the shorter C-terminal fragment 255–316 [10].

2. Materials and methods

Thermolysin was bought from Sigma as a crystallized and lyophilized powder. The C-terminal 255–316 fragment was obtained by autolytic cleavage of the enzyme in the presence of EDTA as described elsewhere [13]. The fragment thus obtained was further purified by reverse-phase HPLC. The homogeneity of the fragment was at least 98%, as checked by SDS-electrophoresis. The concentration of the 205–316 fragment was determined using the $E^{0.1\%}$ coefficient 0.86 at 280 nm [11]. The concentration of the buffers used (glycine, formiate and acetate) was 20 mM and the ionic strength, 0.13 M, was kept constant by the addition of appropriate amounts of NaCl at each pH. All chemicals were of the highest purity available, and distilled, deionized Milli-Q water was used throughout.

Calorimetric experiments were carried out in a DASM-4 instrument with cell volumes of 0.47 ml, under a constant pressure of 2.5 atm, and at heating rates of 0.5, 1.0 and 2.0 K/min. Before being put into the cell the samples were extensively dialyzed against the appropriate buffer solutions. They were routinely heated up to 90–100°C and then cooled inside the calorimeter cell and reheated once more to check for the reversibility of the unfolding. Fragment concentration in DSC experiments was within the range of 0.5 to 4.0 mg/ml. After subtracting the instrumental base line from the original DSC recording, the resulting endotherms were corrected for the effect of the time response of the instrument [14]. The apparent molar partial heat capacity traces were obtained as shown by Privalov and Potekhin [15], using the partial specific volume of the fragment, 0.73 ml/g, calculated from the known sequence of the fragment, and the data of Makhatadze et al. [16]. Thermodynamic molar quantities were obtained using a molecular mass for the fragment of 11 978 Da. The uncertainties in the unfolding temperatures and in the enthalpy values were about 0.1°C and ±5%, respectively.

Sedimentation equilibrium experiments were performed at 10°C using a Beckman XL-A analytical ultracentrifuge, with six-channel 12 mm centrepieces of epon-charcoal. Samples of the 205–316 thermolysin fragment at different concentrations (0.1, 0.5 and 1.0 mg/ml) at each of the three pH values, 2.5, 4.0 and 5.0, were equilibrated at various rotor speeds (20, 25 and 32 krpm). After sedimentation equilibrium was reached radial scans were taken at 280–300 nm.

Relative molecular masses, M_r, were obtained by analyzing the experimental data with programs XLAEQ and EQASSOC supplied by Beckman [17]. The partial specific volume of the fragment was obtained as described above and was corrected for the temperature effect according to Durchschlag [18]. Experimental data at each pH were globally fitted to a monomer-dimer equilibrium model (Eq. (1)), using the ORIGIN version [19] of the NONLIN algorithm [20] supplied by Beckman, with the standard deviation of the absorbance readings as a weighting factor:

$$A(r) = A(r_o)\exp\left[HM_1\left(r^2 - r_o^2\right)\right] + A(r_o)^2 K_2^A \exp\left[2HM_1\left(r^2 - r_o^2\right)\right] + \delta \qquad (1)$$

where $A(r)$ stands for the total protein concentration in absorption units at a given radius, r,; r_o is an arbitrary reference radial distance; $H = (1 - v\rho)\omega^2/2RT$, where v is the partial specific volume of the fragment, ρ is the solution density, ω is the angular velocity of the rotor, R is the gas constant and T the absolute temperature; M_1 is the monomer molecular mass, and δ a baseline offset. The equilibrium constant for the dimer formation, K_2^A, is transformed into the equivalent constant in molar units, K_2^M, by means of the equation $K_2^M = K_2^A \varepsilon l/2$, where ε is the molar absorption coefficient of the fragment and l the path length of the centrifuge cell [21]. The dimerization constants at pH 3.0 and 3.5 were obtained from interpolation of the very good straight fit of ln K_2^M versus pH (results not shown).

3. Results

Differential scanning calorimetry experiments of the 205–316 thermolysin fragment were carried out at pH values 2.5, 3.0, 3.5, 4.0 and 5.0. Within this pH range the unfolding thermal transitions were highly reversible on reheating the samples (> 90%) and independent of scan rate within the range 0.5–2.0 K/min, thus taking place

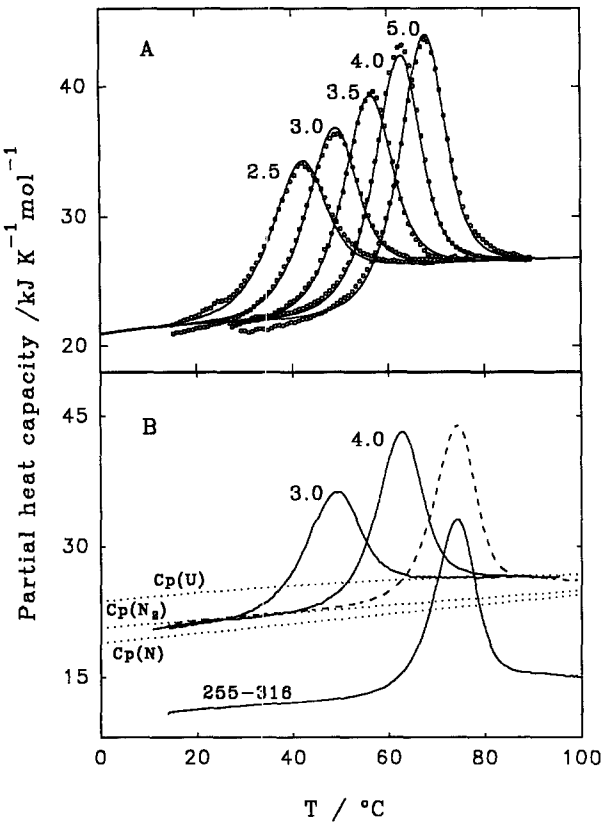

Fig. 1. (A) Temperature dependence of the apparent partial heat capacity of the 205–316 thermolysin fragment at the five pH values indicated in the thermograms: open circles refer to experimental DSC data and solid lines to their best fitting to the model of Eq. (2). (B) The solid bottom curve corresponds to the DSC result of the 255–316 fragment at pH 7.5 (taken from Ref. [10]), whereas the dashed line shows the sum of this curve to the C_p of the unfolded polypeptide chain 205–254 (see text). Dotted lines show the heat capacity of the folded monomer, N, folded dimer, N_2, and unfolded monomer, U, of the 205–316 fragment obtained as described in the text. Experimental solid C_p curves for this fragment at pH 3.0 and 4.0 are also included for purposes of comparison.

under equilibrium conditions in the calorimeter cell. Fig. 1 shows the apparent partial molar heat capacity of the fragment as a function of temperature for this acidic pH range, together with the heat capacity values of the folded dimer, N_2, the folded monomer, N, and the unfolded monomer, U, as well as the result of the fitting of the DSC data according to the following equilibrium model

$$N_2 \overset{K_D}{\rightleftharpoons} 2N \overset{K_U}{\rightleftharpoons} 2U \qquad (2)$$

where K_D stands for the dissociation constant of the dimer and K_U for the unfolding constant of the monomer (see below). The uncertainty in the absolute heat capacity values of the samples at 20°C has been found to be ±2 kJ K^{-1} mol^{-1}. It is evident that the thermal stability of the fragment clearly increases with pH within the range 2.5 to 5.0 (Fig. 1A).

We have calculated the calorimetric parameters of the reversible transitions, such as the calorimetric enthalpy, ΔH, i.e., the area under the DSC peak, using a sigmoidal, chemical base line as described elsewhere [22], and the van't Hoff enthalpy calculated from the equation $\Delta H^{vH} = 4RT_m^2 C_p^m / \Delta H$, where C_p^m stands for the excess C_p value at T_m. In all cases, $\Delta H^{vH} > \Delta H$, indicating that the transition does not correspond to a monomeric two-state process and that there are intermolecular interactions in the folded monomer, i.e., monomer associations. This conclusion also agrees with the observed asymmetrical shape of the transitions [23]. The average value for all experiments of the $\Delta H / \Delta H^{vH}$ ratio is equal to 0.81 ± 0.03. This value is higher than 0.73, the value corresponding to a dimer that unfolds into monomers, as we have shown to be the case for the 255–316 thermolysin fragment [10], and much higher than the values expected for the two-state unfolding of larger association states [15,23].

Fig. 2 shows the effect of fragment concentration on the T_m values of the DSC endotherms within the pH range 2.5–5.0. At all pH values there is a clear concentration effect, that is to say the higher the concentration the higher the T_m value. This result suggests once more the existence of a dissociation equilibrium of the fragment concomitant with its thermal unfolding. Nevertheless, a simple dimer dissociation-unfolding linked process, $N_2 \rightleftharpoons 2U$ (where N_2 and U stand for the folded dimer and the unfolded monomer, respectively), leads to a higher concentration effect than the one shown in Fig. 2 [22,23].

It is clear then that higher association states for the 205–316 fragment at low temperatures would contradict

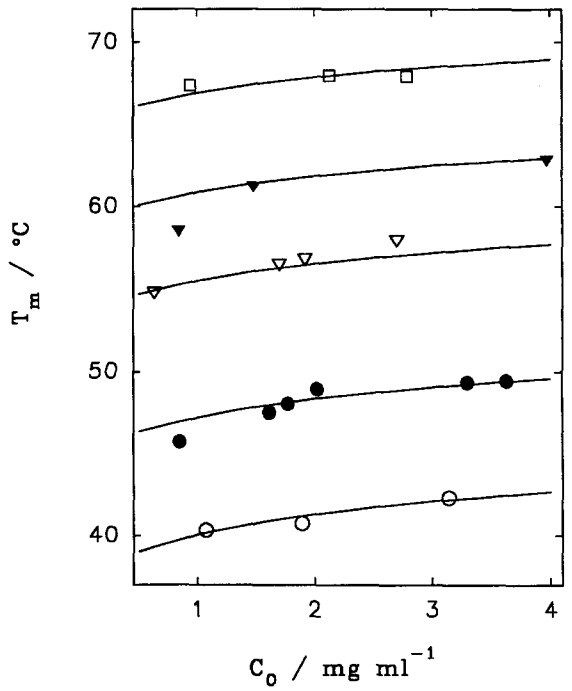

Fig. 2. Concentration dependence of the experimental T_m values for the thermal unfolding of the 205–316 fragment at five pH values: 5.0 (□); 4.0 (▼); 3.5 (▽); 3.0 (●); 2.5 (○). Solid lines show the dependence at each pH according to the global analysis of the DSC results.

even more the above-mentioned enthalpy ratio, as well as the extent of the T_m dependence on sample concentration. Therefore, the simplest plausible model to describe the thermal behaviour of the 205–316 fragment would be that described by a temperature-dependent, folded, monomer-dimer equilibrium which, on temperature increase, would give rise to unfolded monomers as the final state. Such a model is the one depicted in Eq. (2). In order to check whether this model is compatible with our DSC results and, if so, to obtain its characteristic thermodynamic parameters, we have carried out a global, multidimensional fitting of the DSC traces as described below.

The molar fractions, X, of the three species and the equilibrium constants included in Eq. (2), for a given total fragment concentration, C_o, expressed per mol of monomer, can be written as

$$X_{N_2} = 2[N_2]/C_o;\ X_N = [N]/C_o;\ X_U = [U]/C_o; \quad (3)$$

$$K_D = [N]^2/[N_2] = 2X_N^2 C_o/X_{N_2};\ K_U = X_U/X_N. \quad (4)$$

Simple transformations of these equations lead to

$$X_N = \left\{-K_D(1+K_U) + \left[K_D^2(1+K_U)^2 + 8C_oK_D\right]^{1/2}\right\} /4C_o;\ X_U = K_U X_N \quad (5)$$

Taking the dimer, N_2, as the reference state, the excess heat capacity, $\Delta C_p(T)$, over that of the reference state consists of two terms, the excess of the intrinsic C_p over the initial state, δC_p^{int}, and the excess heat absorption of the process(es), δC_p^{ex} [24]:

$$\Delta C_p(T) = \delta C_p^{int} + \delta C_p^{ex} \quad (6)$$

where in this case

$$\delta C_p^{int} = X_N \Delta C_{p,D}/2 + (\Delta C_{p,U} + \Delta C_{p,D}/2) X_U \quad (7)$$

$$\delta C_p^{ex} = \Delta H_D(dX_N/dT)/2 + (\Delta H_U + \Delta H_D/2) \times [K_U(dX_N/dT) + X_N(dK_U/dT)] \quad (8)$$

Here ΔH_D and $\Delta C_{p,D}$ stand for the enthalpy and heat capacity changes of dissociation of the dimer, and ΔH_U and $\Delta C_{p,U}$ for the corresponding values of the monomer unfolding. Derivation of Eq. (5) leads to the value of dX_N/dT, which includes dK_U/dT and dK_D/dT, that can be written as

$$dK_U/dT = K_U \Delta H_U/RT^2;\ dK_D/dT = 2K_D \Delta H_D/RT^2 \quad (9)$$

The functions ΔH, ΔS and ΔC_p for both the dissociation (D) and the unfolding (U) processes can be represented as:

$$\Delta H(T) = \Delta H(T_o) + \int_{T_o}^{T} \Delta C_p(T)dT;$$

$$\Delta S(T) = \Delta S(T_o) + \int_{T_o}^{T} (\Delta C_p(T)/T)dT \quad (10)$$

Here T_o is a reference temperature chosen to be 50°C as an approximate average of the experimental temperature range. The corresponding ΔC_p values are defined by:

$$\Delta C_{p,D} = 2[C_p(N) - C_p(N_2)];\ \Delta C_{p,U} = C_p(U) - C_p(N) \quad (11)$$

where $C_p(N)$, $C_p(N_2)$ and $C_p(U)$ stand for the molar heat capacities of the folded monomer, the folded dimer and the unfolded fragment, respectively, all expressed per mol of monomer.

Finally, the equilibrium constants are obtained by the following equations:

$$\Delta G_D(T) = \Delta H_D(T) - T\Delta S_D(T);$$

$$\Delta G_U(T) = \Delta H_U(T) - T\Delta S_U(T) \quad (12)$$

$$K_D(T) = \exp[-2\Delta G_D(T)/RT];$$

$$K_U(T) = \exp[-\Delta G_U(T)/RT] \quad (13)$$

To fit the experimental molar heat capacity curves to Eqs. (6)–(8), we have firstly obtained an analytical expression for $C_p(U)$ based on a second-order, least-squares regression through the heat capacity data of the elements of protein chemical structure, as reported at several temperatures [25]

$$C_p(U) = -8.9649 + 0.1851T - 0.000239T^2\ (kJ/K \cdot mol) \quad (14)$$

whereas, as usual, we have used linear T functions for the heat capacities of both the folded monomer and the dimer, expressed per mol of monomer

$$C_p(N_2) = a + bT;\ C_p(N) = c + dT \quad (15)$$

Here we have assumed for the sake of simplicity that both straight lines intercept with that of $C_p(U)$ at 140°C, the temperature at which the heat capacity of unfolding has been reported to become zero [26]. Therefore, both $\Delta C_{p,D}$ and $\Delta C_{p,U}$ functions (Eq. (11)) depend upon only two independent adjustable parameters. Finally, we have made the general assumption that neither the heat capacity values, $C_p(N_2)$, $C_p(N)$ and $C_p(U)$, nor the enthalpy changes, $\Delta H_D(T)$ and $\Delta H_U(T)$, depend on pH but on temperature alone [27]. The effect of pH on the stability arises then solely from the different entropy changes at each pH and their influence on the ΔG and K values.

To decrease the number of adjustable parameters in the overall curve fitting we have obtained independently the K_D values at 10°C and different pH values by equilibrium sedimentation experiments (see below), which fix the ΔS_D parameters. For each DSC curve the protein concentration, C_o, is an experimental, known parameter, and, obviously, the more curves (i.e., more experimental information) we use simultaneously in the analysis, the more accurate the fitted parameters that can be obtained. In this way we have carried out a non-linear, multidimensional fitting of the DSC traces at different pH values to the model of Eq. (2),

Table 1
Thermodynamic parameters

ΔH_D (kJ/mol)	ΔH_U (kJ/mol)	C_p(N) (kJ/K · mol)	C_p (N_2) (kJ/K · mol)
3.8	186	21.75	22.88
(−2.4 → 8.6)	(183 → 189)	(21.62 → 21.87)	(22.81 → 22.95)
pH	ΔS_U (kJ/K · mol)		
5.0	0.548 (0.539 → 0.560)		
4.0	0.561 (0.552 → 0.573)		
3.5	0.572 (0.563 → 0.584)		
3.0	0.588 (0.579 → 0.600)		
2.5	0.601 (0.591 → 0.612)		

Thermodynamic parameters obtained from the multidimensional fitting of the partial molar heat capacity curves according to the model developed in the text (Eq. 2) for the 205–316 fragment of thermolysin. Parameters in the Table correspond to T_0 = 50°C. Values in parentheses show the error interval. Values of ΔS_D were fixed in the analysis on the basis of the ultracentrifuge results (see text). All parameters are expressed per mol of monomer.

where only four common parameters for all traces had to be fitted, $C_p(N_2)$, $C_p(N)$, ΔH_D and ΔH_U, in addition to another independent parameter at each of the 5 pH values, ΔS_U, all of them at the reference temperature of 50°C. For the fitting analysis we have developed a specific software based on the optimization Simplex algorithm. We have also made an analysis of variance of the fitting parameters [28] to estimate of their uncertainty. The results of this global fitting are shown in Fig. 1A and Fig. 2 and the corresponding thermodynamic parameters are listed in Table 1.

Sedimentation equilibrium experiments at pH 2.5, 4.0 and 5.0 show that the relative molecular mass of the 205–316 fragment at 0.1 mg/ml (M_r 19000–19800) is higher than that corresponding to the single monomer, 11978, and closer to the dimeric fragment (M_r 22000–24400 at the highest sample concentration employed, 1.0 mg/ml) (data not shown, taken from the low-speed sedimentation equilibrium runs at 20000 rpm). This behaviour, where M_r increases concomitantly with sample concentration, is characteristic of a self-association system [29]. The global analysis of the experimental data at each pH, corresponding to the monomer-dimer equilibrium model is summarized in Table 2 (see also Fig. 3). This analysis indicates that the 205–316 fragment associates with a moderate affinity in the 10^5 M^{-1} range and that the process has little dependence on pH, which would mean that ionizable groups are not likely to be involved in the association.

The temperature dependence of the enthalpy and Gibbs energy changes between the different states of the fragment have been calculated from the set of parameters listed in Table 1, and are shown in Fig. 4. The ΔH of unfolding of both the monomer and the dimer shows the expected positive temperature dependence according to their positive ΔC_p unfolding values. Nevertheless, ΔH_D decreases with temperature, from positive values at low temperature to small negative ones above 50°C, due to the negative sign obtained for $\Delta C_{p,D}$. The ΔG of unfolding for the monomer and dimer attain their maximum values at around 0°C. The dimer has a higher ΔG than that of the

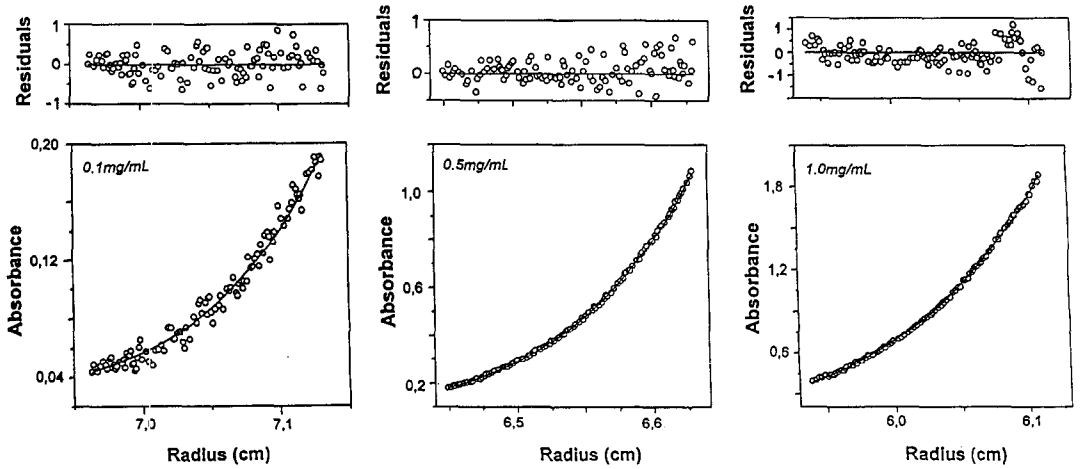

Fig. 3. Radial distribution of concentration and residuals of the 205–316 fragment as a monomer-dimer equilibrium at pH 2.5. Open circles correspond to the experimental data obtained at 25000 rpm, for three different concentrations (0.1, 0.5 and 1.0 mg/ml). The solid line is the best-fit curve of the global analysis to a monomer-dimer equilibrium as described in the text. The results of the fitting are given in Table 2.

Table 2
Dependence on pH of the equilibrium dimerization constant of the 205–316 C-terminal fragment of thermolysin [a]

pH	K_2 [A] (A^{-1}) [b]	rms (A) [c]	K_2^M (M^{-1})
2.5	5.3 (5.0 → 5.8)	0.0095	$6.2 \cdot 10^5$
4.0	3.5 (3.3 → 3.7)	0.0180	$4.1 \cdot 10^5$
5.0	3.1 (2.9 → 3.3)	0.0131	$3.5 \cdot 10^5$

[a] See Section 2 for details of the analysis.
[b] Corrected to 1 cm path length. The values in parentheses correspond to 95% confidence intervals.
[c] Root mean square deviation of the fit in units of absorbance.

monomer at all temperatures, with a minimum difference at about 45°C, at which the dissociation constant is highest (Fig. 4B).

Within the whole set of our dissociation and unfolding parameters, the unusual negative sign of $\Delta C_{p,D}$ is noteworthy. According to the analysis of the experimental data under our DSC conditions, the folded monomer is the least populated species in equilibrium and, therefore, the thermodynamic parameters related to this state have the highest uncertainty. Nevertheless, the estimated error for $\Delta C_{p,D}$ is relatively low (Table 1). In order to test the reliability of our $\Delta C_{p,D}$ value, we have carried out exhaustive simulations of the C_p curves by using the equations of the model and the measured dissociation constants, and have checked the effect of different values and signs for ΔH_D and $\Delta C_{p,D}$ on the simulated C_p curves (results not shown). We should like to point out that a fixed positive, or even zero value for $\Delta C_{p,D}$ precludes any reasonable explanation for our overall DSC data.

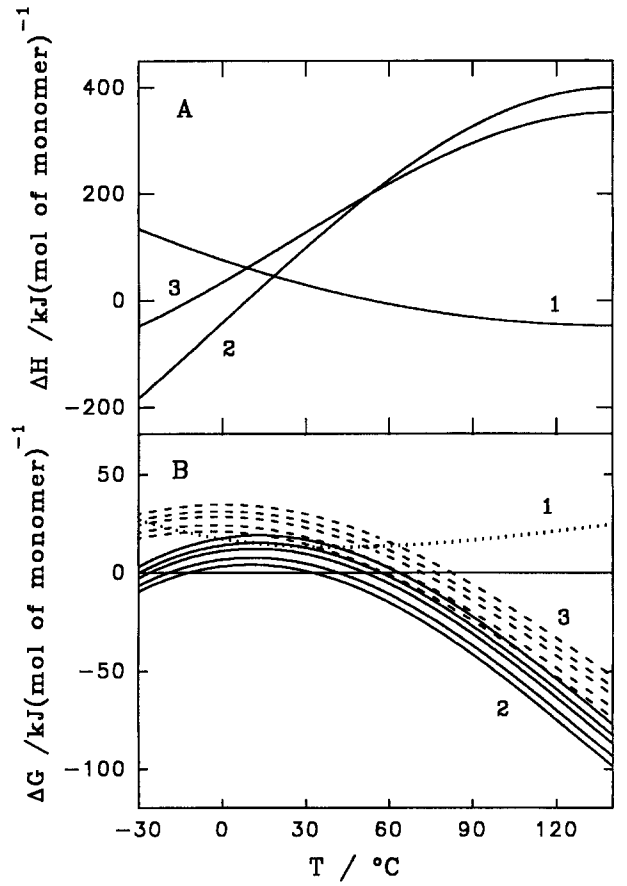

Fig. 4. Temperature dependence of enthalpy (A) and Gibbs energy (B) of dimer dissociation (1), unfolding of the monomer (2) and unfolding of the dimer (3) for the 205–316 fragment of thermolysin. The ΔG functions are shown for the same five pH values as in Figs. 1A and 2, decreasing from top to bottom. The five Gibbs energy curves for the dissociation process appear practically superimposed.

4. Discussion

The 205-316 thermolysin fragment forms a 4 α-helix (233–246, 260–274, 281–296 and 301–313) bundle in native thermolysin, whereas the 255–316 fragment has lost the 233–246 helix and remains as a 3-helix subdomain in the crystal structure of the enzyme [3,4]. We have recently shown [10] that the 255–316 fragment behaves as a compact, globular dimer in solution at pH 7.5, in agreement with sedimentation and NMR studies [11,12], and undergoes a two-state thermal transition, giving rise to unfolded monomers.

Our DSC investigation of the larger 205–316 thermolysin fragment at acidic pH values shows the existence of an equilibrium between folded monomers and dimers, which unfold into isolated monomers. In fact, the experimental DSC traces are predicted quantitatively by the theoretical ones corresponding to the model depicted in Eq. (2). (Fig. 1A). The model also explains satisfactorily the concentration dependence of the T_m values in the pH range 2.5–5.0 (Fig. 2). This has allowed us to obtain thermodynamic information about the monomer, which could not be accessible in the 255–316 fragment, the monomer of which was not significantly populated under the DSC experimental conditions [10]. Vita et al. [11] reported a monomeric character for the 206–316 fragment of thermolysin at pH 7.5, with a significant decrease in the sedimentation coefficient at both acidic and alkaline pH. The difference between our results and those of Vita et al. [11] may be due to the effect of the hydrophobic Met-205 residue, and the fact that they also used a 10-fold lower ionic strength.

The heat capacity change of unfolding of both the folded monomer, $C_p(U) - C_p(N)$, and folded dimer, $C_p(U) - C_p(N_2)$, is positive as expected from the exposure of buried hydrophobic residues upon unfolding (see Fig. 1A, Table 1 and Eq. (11)), although with specific values lower than those of compact globular proteins [27]. This suggests that both conformations have a less compact and/or extensive hydrophobic core in relation to the size of each species. At this point it is interesting to compare the C_p values of this fragment with those of the dimeric 255–316 thermolysin fragment (Fig. 1B). Firstly, the molar C_p change of unfolding is similar for both dimers in spite of

their different size. Secondly, if we add the C_p function of the smaller fragment to the calculated C_p value of the 205–254 difference chain, assuming that this chain is unfolded and using the above-mentioned C_p values [25], we obtain a C_p trace which coincides very well with the experimental one of the 205–316 fragment, both before (folded state) and after (unfolded state) the thermal transition (Fig. 1B). Since the larger fragment is mostly dimeric before the transition, this result is consistent with a rather disordered state for the 205–254 peptide chain in the fragment.

The most striking result is the negative value found for $\Delta C_{p,D}$. The ΔC_p of binding in protein–ligand interactions is usually negative [30–32]. This negative value is larger when binding is coupled to partial or complete protein folding than when binding refers to rigid body associations [1]. Therefore, the only reasonable explanation for our $\Delta C_{p,D}$ value would be that of association coupled to a somewhat partial unfolding, since the burial of non polar surface seems to be the dominant term in the association ΔC_p values versus the change in the polar surface area [1]. In fact, the 255–316, 3-helix fragment is a dimer in solution [10,11], where the interface between the two subunits, of a marked hydrophobic character, coincides topologically with that between the fragment and the rest of the protein in the intact enzyme [12]. Preliminary NMR studies at pH 4 and 5 show that the dimer of the 205–316 fragment is also stabilized by the same favourable 3-helix interaction, leaving the first 233–246 helix and the N-terminal part of the chain close to random conformation (manuscript in preparation). The isolated 233–248 peptide in solution has also been shown by CD and 2-D NMR to have only a 13–17% propensity for helix formation [33]. The fact that the hydrophobic surfaces of about 50 residues are already exposed in the folded dimer would be responsible for its above-mentioned low specific ΔC_p of unfolding. The dissociation of the dimer could give rise to 4-helix bundle monomers with a helix content similar to that of the fragment in native thermolysin. Although further structural studies of the monomeric and dimeric 205–316 fragment are still required, our tentative proposal would explain the negative $\Delta C_{p,D}$ value since on dissociation there would be net apolar surface buried as a result of the formation of the 233–246 α-helix and its docking onto the 3-helix surface that forms the dimer interface.

Fig. 4A shows the temperature dependence of the ΔH values for the dissociation and unfolding processes as obtained from the data in Table 1. The unfolding ΔH of the monomer tends to 400 kJ/mol (3.57 kJ/amino acid residue) at 140°C, whereas that of the dimer tends to 350 kJ/mol (3.12 kJ/residue), both values lower than the value proposed for compact globular proteins at 140°C, 6.25 kJ/residue [26]. This contrasts with the higher ΔH value extrapolated for the 255–316 fragment, 5.80 kJ/residue [10]. This result is again compatible with a partially unfolded or disordered structure for the 205–316 fragment.

Fig. 4B shows the temperature dependence of the ΔG values for unfolding and dissociation of the fragment at different pH values. The stability of the monomer is very low, especially at low pH, which would allow the monomer to undergo cold denaturation at temperatures close to 0°C. Since these transitions would be rather broad because of their low enthalpy, they could be at least partially detected by DSC in the case of high monomer concentration. It is evident that this is not the case, however, because of the stabilizing effect of the fragment association (Fig. 3B). The pH dependence of the ΔG values of dissociation is very low (see Fig. 4B) and can be fitted very well to a straight line (results not shown), according to the equation $(\partial \Delta G/\partial \mathrm{pH})_T = 2.303 RT\nu$, where ν stands for the number of protons taken on dissociation [34]. From the slope of the plot, ν turns out to be only -0.1, which suggests that the process has very little electrostatic character.

Finally, we have shown that the 205–316 thermolysin fragment undergoes a reversible co-operative thermal unfolding, as does the 255–316 fragment. Under DSC experimental conditions the latter seems to behave only as a dimer in solution, whereas the former behaves as monomer-dimer equilibrium. Thus, the presence of the additional 50 amino-acid polypeptide chain in the 205–316 fragment, versus the 255–316 fragment, stabilizes to some extent the folded monomer population in the dissociation equilibrium; the fact that the monomer of the 255–316 fragment is also folded in solution has been shown at very low sample concentration (< 0.1 mg/ml) [11]. We have also shown that the 205–316 fragment has a somewhat less compact conformation than that of the 255–316 fragment. Nevertheless, both fragments are clearly stabilized by their association into dimers in solution.

Acknowledgements

This research has been supported by DGICYT grants PB90-0876 and PB93-1163 from the Ministerio de Educación y Ciencia (Spain). F.C.-L. and A.I.A. acknowledge predoctoral fellowships from the DGICYT and Junta de Andalucía (Spain) respectively. We thank Dr. J.M. Andreu for his help with the analytical ultracentrifugation experiments, Drs. M. Rico and M.A. Jiménez for providing us with unpublished NMR data, and Dr. J. Trout for revising the English text.

References

[1] Spolar, R.S. and Record, M.T., Jr. (1994) Science 263, 777–784.
[2] Wetlaufer, D.B. (1981) Adv. Protein Chem. 34, 61–92.
[3] Matthews, B.W., Weaver, L.H. and Kester, W.R. (1974) J. Biol. Chem. 249, 8030–8044.
[4] Holmes, M.A. and Matthews, B.W. (1982) J. Mol. Biol. 160, 623–639.
[5] Vita, C. and Fontana, A. (1982) Biochemistry 21, 5196–5202.

[6] Vita, C., Dalzoppo, D. and Fontana, A. (1983) Int. J. Pept. Protein Res. 21, 49–56.
[7] Vita, C., Fontana, A. and Chaiken, I.M. (1985) Eur. J. Biochem. 151, 191–196.
[8] Dalzoppo, D., Vita, C. and Fontana, A. (1985) Biopolymers 24, 767–782.
[9] Fontana, A. (1990) in Peptides: Chemistry, Structure and Biology (Rivier, J. and Marshall, G.E., eds.), pp. 557–564, Escom, Leiden.
[10] Conejero-Lara, F., De Filippis, V., Fontana, A. and Mateo, P.L. (1994) FEBS Lett. 344, 154–156.
[11] Vita, C., Fontana, A. and Jaenicke, R. (1989) Eur. J. Biochem. 183, 513–518.
[12] Rico, M., Jimenez, M.A., González, C., De Fillipis, V. and Fontana, A. (1994) Biochemistry 33, 14834–14847.
[13] Fassina, G., Vita, C., Dalzoppo, D., Zamai, M., Zambonin, M and Fontana, A. (1986) Eur. J. Biochem. 156, 221–228.
[14] López-Mayorga, O. and Freire, E. (1987) Biophys. Chem. 87, 87–96.
[15] Privalov, P.L. and Potekhin, S.V. (1986) Methods Enzymol. 114, 4–51.
[16] Makhatadze, G.I., Medvedkin, V.N. and Privalov, P.L. (1990) Biopolymers 30, 1001–1010.
[17] Minton, A.P. (1994) in Modern Analytical Ultracentrifugation (Schuster, T.M. and Laue, T.M., eds.), pp. 81–93. Birkhäuser, Boston, MA.
[18] Durchschlag, H. (1986) in Thermodynamic Data for Biochemistry and Biotechnology (Hinz, H.J., ed.), pp. 45–128, Springer, Berlin.
[19] Hedges, J., Sarrafzadeh, S., Lear, J.D. and McRorie, D.K. (1984) in Modern Analytical Ultracentrifugation (Schuster, T.M. and Laue, T.M., eds.), pp. 227–244, Birkhäuser, Boston, MA.
[20] Johnson, M.L., Correa, J.J., Yphantis, D.A. and Halvorson, H.R. (1981) Biophys. J. 36, 575–588.
[21] Lewis, M.S. (1991) Biochemistry 30, 11716–11718.
[22] Takahashi, K. and Sturtevant, J.M. (1981) Biochemistry 20, 6185–6190.
[23] Freire, E. (1989) Comments Mol. Cell. Biophys. 6, 123–140.
[24] Viguera, A.R., Martínez, J.C., Filimonov, V.V., Mateo, P.L. and Serrano, L. (1994) Biochemistry 33, 2142–2150.
[25] Makhatadze, G.I. and Privalov, P.L. (1990) J. Mol. Biol. 213, 375–384.
[26] Privalov, P.L. and Gill, S.J. (1988) Adv. Protein Chem. 39, 191–234.
[27] Privalov, P.L. (1979) Adv. Protein Chem. 33, 167–241.
[28] Bevington, P.R. (1969) in Data Reduction and Error Analysis for the Physical Sciences, McGraw-Hill, New York.
[29] MacRorie, D.K. and Voelker, P.J. (1993) Self-Associating Systems in the Analytical Ultracentrifuge, Beckman Instruments Inc., Palo Alto, CA.
[30] Sturtevant, J.M. (1977) Proc. Natl. Acad. Sci. USA 74, 2236–2240.
[31] Wiesinger, H. and Hinz, H.J. (1987) in Thermodynamic Data for Biochemistry and Biotechnology (Hinz, H.J., ed.), pp. 211–226, Springer, Berlin.
[32] Ross, P.D. (1987) in Thermodynamic Data for Biochemistry and Biotechnology (Hinz, H.J., ed.), pp. 227–233, Springer, Berlin.
[33] Jimenez, M.A., Bruix, M., González, C., Blanco, F.J., Nieto, J.L., Herranz, J. and Rico, M. (1993) Eur. J. Biochem. 211, 569–581.
[34] Hinz, H.J., Shiao, D.D.F. and Sturtevant, J.M. (1971) Biochemistry 10, 1347–1352.